

## QUANTUM GROUP ON A HONEYCOMB LATTICE

M. ELIASHVILI, G. JAPARIDZE AND G. TSITSISHVILI

**ABSTRACT.** The tight-binding model of electrons on a honeycomb lattice is studied in the presence of a homogeneous magnetic field. Provided the magnetic flux per unit hexagon is rational of the elementary flux the one-particle Hamiltonian is expressed in terms of the generators of the quantum group  $U_q(sl_2)$ . Employing the functional representation of  $U_q(sl_2)$  the Harper equation is rewritten as a systems of two coupled functional equations on a complex plane. For the special values of quasi-momentum the entangled system admits solutions in terms of polynomials. In that case the system exhibits certain symmetry relations allowing to resolve the entanglement, and basic single equation determining the eigenvalues and eigenstates (polynomials) is obtained. Equations specifying the locations of the roots of polynomials on a complex plane and consequently the one-particle wave functions are found. Employing numeric analysis the roots of polynomials corresponding to different eigenstates are solved out and the diagrams exhibiting the ordered structure of one-particle states are depicted.

**რეზიუმე.** განხილულია ფიჭურ მესერზე აგებული ელექტრონული სისტემის ჰამილტონის ოპერატორის დიაგონალიზების ამოცანა მაგნიტური ველის პირობებში. შესწავლილია შემთხვევა, როდესაც ელემენტარულ ექვსკუთხედში მაგნიტური ნაკადი წარმოადგენს მაგნიტური ნაკადის კვანტის რაციონალურ ნაწილს. ამ პირობის გათვალისწინებით სისტემის ჰამილტონიანი გამოხატულია  $U_q(sl_2)$  კვანტური ჯგუფის გენერატორების მეშვეობით. გამოყენებულია კვანტური ჯგუფის ფუნქციონალური წარმოდგენა და საკუთრივი რიცხვების ამოცანა დაყვანილია ფუნქციონალურ განტოლებებზე, რომელსაც გააჩნია ამოხსნები ნამდვილ პოლინომთა სივრცეში. აქედან გამომდინარე, ყოველი საკუთარი ვექტორი ხასიათდება შესაბამისი პოლინომის ნულების მეშვეობით. მიღებულია განტოლება, რომელიც განსაზღვრავს ამ ნულების განლაგებას კომპლექსურ სიბრტყეზე. რიცხვითი მეთოდების გამოყენებით გამოთვლილია ასეთი ნულების კონკრეტული მნიშვნელობები სისტემის მახასიათებელი სიდიდეების სხვადასხვა მნიშვნელობებისათვის. ნულების განაწილება კომპლექსურ სიბრტყეზე წარმოდგენილია გრაფიკულად, საიდანაც ნათლად ჩანს ნულების განლაგებისა, და შესაბამისად, სისტემის ჰამილტონის საკუთარი ვექტორების არატრივიალური და მოწესრიგებული სტრუქტურა.

---

2010 *Mathematics Subject Classification.* 81T25, 81R50.

*Key words and phrases.* Quantum group, honeycomb lattice, functional equation.

## 1. INTRODUCTION

The problem of two-dimensional electrons moving in a periodic potential and a uniform magnetic field has been the subject of intensive studies for decades. Azbel [1] was the first who pointed out that the spectral properties of the two-dimensional lattice electrons have a sensitive dependence on the flux through the plaquette. Later this observation has been developed by Hofstadter [2] who found the exotic structure of the one-particle energy spectrum of the system of planar electrons on square lattice in magnetic field. The same study was extended later for the triangular lattice [3], generalized square lattices [4, 5] and for the honeycomb lattice [6, 7]. These studies firmly established the fractal structure of the aforementioned energy spectrum, whose rich and complex nature originates from the presence of two, not necessarily commensurate periods. The first is given by the lattice structure and the second is determined by the magnetic field. The relevant parameter which determines the band structure is the ratio  $\Phi/\Phi_0$  where  $\Phi$  is the magnetic flux per elementary hexagon, and  $\Phi_0 = 2\pi(\hbar/e)$  is the flux quantum.

In 1994 Wiegmann and Zabrodin pointed out [8] that the Hamiltonian responsible for the original result of Hofstadter is closely related to the quantum group  $U_q(sl_2)$  (for mathematical treatment see [9]). Namely, it was shown, that the Hamiltonian is expressible in terms of  $X^\pm$  generators of quantum group  $U_q(sl_2)$ :  $\mathcal{H} = X^+ + X^-$  with the deformation parameter  $q$  determined by the applied magnetic field. Employing the functional representation of  $U_q(sl_2)$  in the space of polynomials, the Harper equation is reformulated into the functional form where the one-particle eigenstates appeared as polynomials. The zeros of polynomials unambiguously specifying the one-particle wave functions were shown to be determined by the Bethe ansatz equations [8]. The fact that eigenstates are related to certain polynomials associated with the quantum group  $U_q(sl_2)$  and with the Bethe ansatz equations provides with possibility to systematically study the structure of eigenstates. It should be noted that so far the studies were mainly concentrated on the structure of spectrum.

Hatsugai *et al.* [10] investigated the Bethe ansatz equations derived in [8] and found out that the zeros of those polynomial are not scattered randomly, but are located along concentric circles on the complex plane. This can be considered as an indication that eigenstates also exhibit nontrivial and ordered structure.

Alongside with the eigenvalue problem for electrons on a square lattice in magnetic field, the analogous problem has been studied for a honeycomb lattice as well [6, 7]. The common observation is that the energy spectrum differs from the one of square lattice and is still highly nontrivial. After the connection between the quantum group  $U_q(sl_2)$  and the problem of square

lattice electrons in magnetic field was found out in [8], the similar approach has been applied to honeycomb lattice by Kohmoto and Sedrakyan [11].

In contrast to the square lattice, the honeycomb is not a Bravais lattice, but consists of two interpenetrating triangular lattices (“ $A$ ” and “ $B$ ” sublattices) with one lattice point of each type per unit cell. Therefore the one-particle Hamiltonian carries additional  $(2 \times 2)$ -matrix structure. In terms of the generators of  $U_q(sl_2)$  it appears as

$$\mathcal{H} = \begin{pmatrix} 0 & \mathbb{1} + X^- \\ \mathbb{1} + X^+ & 0 \end{pmatrix} \quad (1)$$

and carries the anti-diagonal structure in  $(2 \times 2)$ -matrix indices. This causes extra inconvenience which can be overcome by considering  $\mathcal{H}^2$  instead of  $\mathcal{H}$  since the former is diagonal in  $(2 \times 2)$ -matrix indices. Taking advantage of this observation, the authors of [11] obtained the analog of the Bethe ansatz equation derived for square lattice [8].

The Hamiltonian (1) describes electrons hopping from a site to the nearest neighboring ones. The squared operator  $\mathcal{H}^2$  contains second-order terms describing double-hoppings  $A \rightarrow B \rightarrow A$  and  $B \rightarrow A \rightarrow B$ . The corresponding Bethe-like equations are relatively complex and the nesting procedure is proposed with the aim to reduce them to the set of simpler equations [11].

In this paper we develop alternative approach to the eigenvalue problem for the Hamiltonian (1). Tracing out certain symmetry of  $\mathcal{H}$  we derive functional equation describing electron hoppings to the nearest sites what is the basic process encoded in  $\mathcal{H}$ . Note, that this equation includes as a corollary the corresponding equation studied in [11].

The paper is organized as follows. In the forthcoming section we present the derivation of one-particle Hamiltonian from the tight-binding model on honeycomb lattice in magnetic field. In Section III we rewrite the one-particle Hamiltonian in terms of the quantum group  $U_q(sl_2)$  and comment on the representations of  $U_q(sl_2)$ . Section IV deals with Harper equation in polynomial representation. Since the honeycomb consists of two triangle Bravais sublattices, the Harper equation appears in the form of the system of two coupled equations. This system obeys certain symmetry property which allows to decouple them and to obtain a single equation describing the elementary process of nearest neighbouring hopping. Solutions to this equation are polynomials with real coefficients and Bethe-like equations determining the zeros of polynomials are derived. In Section V the results of numerical analysis are presented and the locations of the zeros on the complex plane are depicted exhibiting nontrivial and ordered structure of eigenstates.

## 2. SPINLESS FERMIONS ON A HONEYCOMB LATTICE IN MAGNETIC FIELD

The honeycomb lattice is made up of the two-dimensional array of hexagonal unit cells, of side  $a$ , with atoms at the vertices. Such a structure is encountered in solid state physics in various crystals, while the ideal realization of the two-dimensional honeycomb lattice is graphene [12]. The unit cell is a rhombus of the side  $a\sqrt{3}$  with angles  $\pi/3$  and  $2\pi/3$  at its vertices. There are two atoms (see Figure 1) in each unit cell,  $A$  and  $B$ .

We consider the tight-binding model of spinless fermions on a honeycomb lattice with the nearest neighbouring hoppings only. In the presence of homogeneous magnetic field the Hamiltonian under consideration is given by

$$H = \sum_{n, \mathbf{r}} \left[ e^{i\gamma_n(\mathbf{r})} c_A^\dagger(\mathbf{r}) c_B(\mathbf{r} + \boldsymbol{\delta}_n) + h.c. \right], \quad (2)$$

where the summation is implied over  $\mathbf{r} = j_1 \mathbf{a}_1 + j_2 \mathbf{a}_2$ . Here  $c_A^\dagger(\mathbf{r})$  ( $c_A(\mathbf{r})$ ) and  $c_B^\dagger(\mathbf{r} + \boldsymbol{\delta}_n)$  ( $c_B(\mathbf{r} + \boldsymbol{\delta}_n)$ ) are the spinless fermion creation (annihilation) operators on site  $\mathbf{r}$  of the sublattice “A” and on site  $\mathbf{r} + \boldsymbol{\delta}_n$  of the sublattice “B”, respectively.

Magnetic field  $\mathcal{B}$  is included in the Hamiltonian via the Peierls phases

$$\gamma_n(\mathbf{r}) = \frac{e}{\hbar} \int_{\mathbf{r}}^{\mathbf{r} + \boldsymbol{\delta}_n} \boldsymbol{\mathcal{A}} dl, \quad (3)$$

where the vector-potential is taken in the Landau gauge  $\boldsymbol{\mathcal{A}} = (-\mathcal{B}y, 0)$ . We put  $e\mathcal{B} < 0$  in what follows.

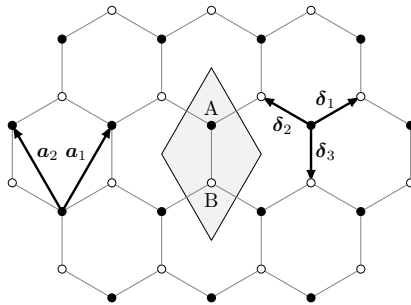


FIGURE 1. Locations of A-sites are set by  $\mathbf{r} = j_1 \mathbf{a}_1 + j_2 \mathbf{a}_2$  where  $\mathbf{a}_{1,2} = \frac{1}{2}(\pm 1, \sqrt{3})a$  and  $j_{1,2}$  integers. The three B-sites, nearest to a given A-site are located at  $\mathbf{r} + \boldsymbol{\delta}_{1,2,3}$ .

Rewriting (2) in the Fourier representation we find

$$\begin{aligned}
 H = & \int_{\text{FBZ}} \left[ e^{i\mathbf{k}\mathbf{a}_1} c_A(\mathbf{k} + \mathbf{k}_0) c_B^\dagger(\mathbf{k}) + h.c. \right] d\mathbf{k} + \\
 & + \int_{\text{FBZ}} \left[ e^{i(\mathbf{k}-\mathbf{k}_0)\mathbf{a}_2} c_A(\mathbf{k} - \mathbf{k}_0) c_B^\dagger(\mathbf{k}) + h.c. \right] d\mathbf{k} + \\
 & + \int_{\text{FBZ}} \left[ c_A^\dagger(\mathbf{k}) c_B(\mathbf{k}) + h.c. \right] d\mathbf{k}, \tag{4}
 \end{aligned}$$

where  $c_A(\mathbf{k})$  and  $c_B(\mathbf{k})$  are the Fourier transforms of  $c_A(\mathbf{r})$  and  $c_B(\mathbf{r} + \boldsymbol{\delta}_n)$  respectively, and the integration covers the first Brillouin zone (FBZ).

The vector  $\mathbf{k}_0$  is related to the magnetic field

$$\mathbf{k}_0 = -\frac{ea\mathcal{B}}{2\hbar} (0, 1) = \frac{2\pi}{\sqrt{3}a} \frac{\Phi}{\Phi_0} (0, 1). \tag{5}$$

We consider

$$\frac{\Phi}{\Phi_0} = \frac{\nu}{N}, \tag{6}$$

where  $\nu$  and  $N$  are coprime integers. Then the Hamiltonian (4) can be presented as follows (see Appendix A)

$$H = \int_{\text{MBZ}} \Psi^\dagger(\mathbf{k}) \mathcal{H}(\mathbf{k}) \Psi(\mathbf{k}) d\mathbf{k}, \tag{7a}$$

$$\mathcal{H}(\mathbf{k}) = \begin{pmatrix} 0 & \mathbb{1} + X^-(\mathbf{k}) \\ \mathbb{1} + X^+(\mathbf{k}) & 0 \end{pmatrix}, \tag{7b}$$

where  $\Psi(\mathbf{k})$  is a  $(2N)$ -component column, and the integration covers the magnetic Brillouin zone, which is the  $\frac{1}{N}$ 'th part of the first Brillouin zone.

The  $N \times N$  matrices  $X^\pm(\mathbf{k})$  are given by

$$X^+(\mathbf{k}) = e^{-i\mathbf{k}\mathbf{a}_1} \beta^\dagger Q + e^{-i\mathbf{k}\mathbf{a}_2} Q \beta, \tag{8a}$$

$$X^-(\mathbf{k}) = e^{+i\mathbf{k}\mathbf{a}_1} Q^\dagger \beta + e^{+i\mathbf{k}\mathbf{a}_2} \beta^\dagger Q^\dagger, \tag{8b}$$

where

$$\beta = \begin{pmatrix} 0 & 1 & 0 & \cdots & 0 & 0 \\ 0 & 0 & 1 & \cdots & 0 & 0 \\ 0 & 0 & 0 & \cdots & 0 & 0 \\ \vdots & \vdots & \vdots & & \vdots & \vdots \\ 0 & 0 & 0 & \cdots & 0 & 1 \\ 1 & 0 & 0 & \cdots & 0 & 0 \end{pmatrix} \tag{9}$$

and

$$Q = \text{diag}(q^1, q^2, \dots, q^N) \tag{10}$$

with

$$q = e^{+i\pi(\nu/N)}. \quad (11)$$

### 3. THE QUANTUM GROUP $U_q(sl_2)$

Using the relation  $Q^\dagger \beta Q = q^2 Q \beta Q^\dagger$  we find

$$[X^+, X^-] = i^2(q - q^{-1})(K - K^{-1}), \quad (12a)$$

$$K X^\pm K^{-1} = q^{\pm 2} X^\pm, \quad (12b)$$

where

$$K(\mathbf{k}) = q e^{+i\mathbf{k}(\mathbf{a}_1 - \mathbf{a}_2)} Q \beta Q^\dagger \beta, \quad (13a)$$

$$K^{-1}(\mathbf{k}) = q^{-1} e^{-i\mathbf{k}(\mathbf{a}_1 - \mathbf{a}_2)} \beta^\dagger Q \beta^\dagger Q^\dagger. \quad (13b)$$

Relations (12) constitute the definition of the quantum group  $U_q(sl_2)$  [13] (we use the normalization for  $X^\pm$  slightly different from the standard one). Remark that (12) are valid irrespectively of the particular values of  $\mathbf{k}$  and  $\mathbf{a}_{1,2}$ .

**3.1. Cyclic and highest weight representations.** In this subsection we bring some details on the cyclic and highest weight representations of  $U_q(sl_2)$ . Below we discuss the case of  $\nu = \text{even}$  to ensure the method (case  $\nu = \text{odd}$  will be considered elsewhere).

Introduce the states  $\psi_1, \psi_2, \dots, \psi_N$  in the form of the  $N$ -component columns

$$\psi_j = N^{-\frac{1}{2}} \{q^j, q^{2j}, q^{3j}, \dots, q^{Nj}\}^T. \quad (14)$$

These vectors form the orthonormal complete set of states

$$\sum_{n=1}^N (\psi_i^\dagger)_n (\psi_j)_n = \delta_{ij}, \quad (15a)$$

$$\sum_{j=1}^N (\psi_j^\dagger)_m (\psi_j)_n = \delta_{mn} \quad (15b)$$

and can be used as a basis in the space of representation.

The action of matrices  $\beta$  and  $Q$  on the states (14) is expressed by the following relations

$$\beta \psi_j = q^j \psi_j, \quad (16a)$$

$$\beta^\dagger \psi_j = q^{-j} \psi_j, \quad (16b)$$

$$Q \psi_j = \psi_{j+1}, \quad (16c)$$

$$Q^\dagger \psi_j = \psi_{j-1}, \quad (16d)$$

where the cyclic identifications  $\psi_{N+j} = \psi_j$  is understood in (16c) and (16d). Later is possible due to  $q^N = 1$ .

Using (16) we find

$$X^+\psi_j = q^{-\frac{1}{2}}e^{-\frac{i}{2}\sqrt{3}k_y a}t_{j+1}\psi_{j+1}, \quad (17a)$$

$$X^-\psi_j = q^{+\frac{1}{2}}e^{+\frac{i}{2}\sqrt{3}k_y a}t_j\psi_{j-1}, \quad (17b)$$

$$K\psi_j = e^{+ik_x a}q^{+2j}\psi_j, \quad (17c)$$

$$K^{-1}\psi_j = e^{-ik_x a}q^{-2j}\psi_j, \quad (17d)$$

where

$$t_j = e^{+\frac{i}{2}k_x a}q^{j-\frac{1}{2}} + e^{-\frac{i}{2}k_x a}q^{-j+\frac{1}{2}}. \quad (18)$$

Due to (17a) and (17b) the operators  $X^+$  and  $X^-$  can be regarded as rising and lowering ones respectively.

From (17a) and (17b) we find

$$\text{Det}X^\pm = q^{\mp\frac{1}{2}N}e^{\mp\frac{i}{2}N\sqrt{3}k_y a}(t_1 t_2 \cdots t_N). \quad (19)$$

For those values of  $k_x$  when  $t_j \neq 0$  for all  $j$ , the operators  $X^\pm$  possess only non-vanishing eigenvalues. In other words, there is neither highest nor lowest weight states. Hence (8) and (13) form the cyclic representation of (12). Acting on  $\psi_j$  by  $X^+$  we obtain  $\psi_{j+1}$ , and so on until we come to  $\psi_N$ . The subsequent action takes us back to  $\psi_1$ . The similar is true for  $X^-$ .

On the other hand, for the specific value of  $k_x$ , one of  $t_1, \dots, t_N$  vanishes. For example, setting  $e^{ik_x a} = -q$  we obtain that  $t_1 = t_{N+1} = 0$ . Then (17a) and (17b) yield  $X^+\psi_N = 0$  and  $X^-\psi_1 = 0$  so that  $\psi_N$  and  $\psi_1$  appear now as the highest and the lowest weight vectors, respectively.

We should remark here on an important detail: as we see, depending on the values of the momentum, the cyclic and the highest weight representations can be switched one to another. Such an interplay has been known for a long time [14].

**3.2. Functional representation.** Consider an  $N$ -component vector  $f = (f_1, f_2, \dots, f_N)$ . Writing out the action of  $X^\pm(\mathbf{k})$  and  $K^{\pm 1}(\mathbf{k})$  on  $f$  in the component form we obtain

$$(X^+f)_n = e^{-i\mathbf{k}\mathbf{a}_1}q^{n-1}f_{n-1} + e^{-i\mathbf{k}\mathbf{a}_2}q^n f_{n+1}, \quad (20a)$$

$$(X^-f)_n = e^{+i\mathbf{k}\mathbf{a}_1}q^{-n}f_{n+1} + e^{+i\mathbf{k}\mathbf{a}_2}q^{-n+1}f_{n-1}, \quad (20b)$$

$$(Kf)_n = e^{+i\mathbf{k}(\mathbf{a}_1 - \mathbf{a}_2)}f_{n+2}, \quad (20c)$$

$$(K^{-1}f)_n = e^{-i\mathbf{k}(\mathbf{a}_1 - \mathbf{a}_2)}f_{n-2}, \quad (20d)$$

where the identification  $f_{N+n} = f_n$  is implied.

Introduce the interpolating function of complex variable  $f(z)$  such that

$$f_n = f(e^{-\frac{i}{2}\sqrt{3}k_y a}q^{n-\frac{1}{2}}). \quad (21)$$

Then the relations (20) can be written as

$$X^+ f(z) = e^{-\frac{i}{2}k_x a} q^{-\frac{1}{2}} z f(q^{-1}z) + e^{+\frac{i}{2}k_x a} q^{+\frac{1}{2}} z f(qz), \quad (22a)$$

$$X^- f(z) = e^{+\frac{i}{2}k_x a} q^{-\frac{1}{2}} z^{-1} f(qz) + e^{-\frac{i}{2}k_x a} q^{+\frac{1}{2}} z^{-1} f(q^{-1}z), \quad (22b)$$

$$K f(z) = e^{+ik_x a} f(q^2 z), \quad (22c)$$

$$K^{-1} f(z) = e^{-ik_x a} f(q^{-2} z). \quad (22d)$$

These relations determine the functional representation of  $U_q(sl_2)$ .

#### 4. THE EIGENVALUE EQUATION

We study the eigenvalue equation

$$\begin{pmatrix} 0 & \mathbb{I} + X^-(\mathbf{k}) \\ \mathbb{I} + X^+(\mathbf{k}) & 0 \end{pmatrix} \begin{pmatrix} \xi \\ \zeta \end{pmatrix} = E \begin{pmatrix} \xi \\ \zeta \end{pmatrix}. \quad (23)$$

Employing the functional representation (22) the eigenvalue equation (23) can be rewritten in the form of two coupled equations

$$\xi(z) + e^{+\frac{i}{2}k_x a} q^{+\frac{1}{2}} z \xi(qz) + e^{-\frac{i}{2}k_x a} q^{-\frac{1}{2}} z \xi(q^{-1}z) = E \zeta(z), \quad (24a)$$

$$\zeta(z) + e^{+\frac{i}{2}k_x a} q^{-\frac{1}{2}} z^{-1} \zeta(qz) + e^{-\frac{i}{2}k_x a} q^{+\frac{1}{2}} z^{-1} \zeta(q^{-1}z) = E \xi(z). \quad (24b)$$

The main disadvantage in resolving (24) is the entanglement of  $\xi(z)$  and  $\zeta(z)$ , and the appropriate way is to decouple the sought for functions. This can be done by applying  $\mathbb{I} + X^-$  to (24a) and  $\mathbb{I} + X^+$  to (24b) thus leading to ( $\varphi = k_x a$ )

$$\begin{aligned} 3\xi(z) + e^{+i\varphi} q \xi(q^2 z) + e^{-i\varphi} q^{-1} \xi(q^{-2} z) + e^{+\frac{i}{2}\varphi} q^{-\frac{1}{2}} \left( \frac{1}{z} + qz \right) \xi(qz) + \\ + e^{-\frac{i}{2}\varphi} q^{+\frac{1}{2}} \left( \frac{1}{z} + q^{-1}z \right) \xi(q^{-1}z) = E^2 \xi(z), \end{aligned} \quad (25a)$$

$$\begin{aligned} 3\zeta(z) + e^{+i\varphi} q^{-1} \zeta(q^2 z) + e^{-i\varphi} q \zeta(q^{-2} z) + e^{+\frac{i}{2}\varphi} q^{-\frac{1}{2}} \left( \frac{1}{z} + qz \right) \zeta(qz) + \\ + e^{-\frac{i}{2}\varphi} q^{+\frac{1}{2}} \left( \frac{1}{z} + q^{-1}z \right) \zeta(q^{-1}z) = E^2 \zeta(z). \end{aligned} \quad (25b)$$

Equations (25) have been studied in [11] where the nesting procedure is applied with the aim to reduce them to the set of simpler equations. Remark, that in that paper the  $\Theta$ -function representation is employed without restricting the values of  $\mathbf{k}$ . In this scope the representation of  $U_q(sl_2)$  used in [11] is cyclic. Remind, that in the paper [8] it is stated, that for a square lattice the relevant representation is a highest weight one.

We now derive the equation describing the elementary process of the nearest site hoppings. For this purpose we first reduce the functional representation to the polynomial representation. Consider monomials  $f_j(z) = z^j$

as the basis in the space of analytic functions. We then find

$$X^+ f_j(z) = t_{j+1} f_{j+1}(z), \quad (26a)$$

$$X^- f_j(z) = t_j f_{j-1}(z), \quad (26b)$$

$$K f_j(z) = q^{+2j} f_j(z), \quad (26c)$$

$$K^{-1} f_j(z) = q^{-2j} f_j(z), \quad (26d)$$

where  $t_j$  has been defined by (18).

The action of  $X^\pm$  can be expressed as

$$\cdots \begin{array}{c} \xrightarrow{X^+} \\ \xleftarrow{X^-} \end{array} f_j \begin{array}{c} \xrightarrow{X^+} \\ \xleftarrow{X^-} \end{array} f_{j+1} \begin{array}{c} \xrightarrow{X^+} \\ \xleftarrow{X^-} \end{array} \cdots . \quad (27)$$

Taking  $e^{ik_x a} = -q$  we find  $X^- f_0 = X^+ f_{N-1} = 0$  *i.e.* the chain (27) breaks down at  $j = 0$  and  $j = N - 1$  respectively. Then the subspace of  $(N-1)$ 'th order polynomials  $f(z) = c_0 + c_1 z + \cdots + c_{N-1} z^{N-1}$  is the invariant subspace and the equations (24) can be resolved in terms of  $(N-1)$ 'th order polynomials.

Provided we set  $e^{ik_x a} = -q$  the system (24) appears as

$$\xi(z) + iqz\xi(qz) - iq^{-1}z\xi(q^{-1}z) = E\zeta(z), \quad (28a)$$

$$\zeta(z) + iz^{-1}\zeta(qz) - iz^{-1}\zeta(q^{-1}z) = E\xi(z). \quad (28b)$$

Remark that (28) admits solutions not merely in terms of polynomials, but in terms of real polynomials, *i.e.* with real coefficients. This can be verified by expanding  $\xi(z)$  and  $\zeta(z)$  in a series of  $z^j$  and rewriting (28) for the expansion coefficients.

Now it is important to remark, that equations (28a) and (28b) are related one to another by the symmetry transformation

$$\zeta(z) \Leftrightarrow z^{2J}\xi(-z^{-1}), \quad (29a)$$

where  $2J = N - 1$ .

Note, that this observation is the key point of our consideration allowing to present the solution to (28) as

$$\begin{pmatrix} \xi(z) \\ \zeta(z) \end{pmatrix} = \begin{pmatrix} f(z) \\ +z^{2J}f(-z^{-1}) \end{pmatrix} \quad E = +\lambda, \quad (30a)$$

$$\begin{pmatrix} \xi(z) \\ \zeta(z) \end{pmatrix} = \begin{pmatrix} f(z) \\ -z^{2J}f(-z^{-1}) \end{pmatrix} \quad E = -\lambda, \quad (30b)$$

where the function  $f(z)$  satisfies the equation

$$f(z) + iqz f(qz) - iq^{-1}z f(q^{-1}z) = \lambda z^{2J} f(-z^{-1}) \quad (31)$$

generating  $N$  eigenvalues  $\lambda_1, \lambda_2, \dots, \lambda_N$ .

Since  $f(z)$  is a polynomial we can write down

$$f(z) = \prod_{j=1}^{2J} (z - z_j), \quad (32)$$

where  $z_1, z_2, \dots, z_{2J}$  are the zeros of  $f(z)$ .

Substituting (32) into (31) and setting  $z = -z_n^{-1}$  we obtain

$$iz_n = \prod_{j=1}^{2J} \frac{1 + qz_n z_j}{1 + z_n z_j} - \prod_{j=1}^{2J} \frac{1 + q^{-1} z_n z_j}{1 + z_n z_j}. \quad (33)$$

The last equation is the honeycomb analog of the Bethe ansatz equation obtained in [8] for square lattice. Due to the fact that (28) is soluble in terms of real polynomials, the solutions to the equation (31) are also real polynomials. Correspondingly, if  $z_n$  is a root then  $z_n^*$  must be the root as well. This agrees with the invariance of (33) under the complex conjugation.

Setting  $z = z_n$ ,  $z = qz_n$  and  $z = q^{-1}z_n$  in (31) we find

$$\lambda \prod_{j=1}^{2J} (1 + z_n z_j) = iqz_n \prod_{j=1}^{2J} (qz_n - z_j) - iq^{-1}z_n \prod_{j=1}^{2J} (q^{-1}z_n - z_j), \quad (34a)$$

$$\lambda \prod_{j=1}^{2J} (1 + qz_n z_j) = \prod_{j=1}^{2J} (qz_n - z_j) + iq^2 z_n \prod_{j=1}^{2J} (q^2 z_n - z_j), \quad (34b)$$

$$\lambda \prod_{j=1}^{2J} (1 + q^{-1} z_n z_j) = \prod_{j=1}^{2J} (q^{-1} z_n - z_j) - iq^{-2} z_n \prod_{j=1}^{2J} (q^{-2} z_n - z_j). \quad (34c)$$

Expressing the products standing in (33) in terms of (34) we obtain the equation

$$\begin{aligned} -q^2 \prod_{j=1}^{2J} (q^2 z_n - z_j) - q^{-2} \prod_{j=1}^{2J} (q^{-2} z_n - z_j) + i \left( \frac{1}{z_n} + qz_n \right) \prod_{j=1}^{2J} (qz_n - z_j) - \\ - i \left( \frac{1}{z_n} + q^{-1} z_n \right) \prod_{j=1}^{2J} (q^{-1} z_n - z_j) = 0. \end{aligned} \quad (35)$$

This equation is the same as (25a) for the value  $z = z_n$ .

Rewriting (31) as

$$\lambda = \prod_{j=1}^{2J} \frac{z - z_j}{1 + zz_j} + iqz \prod_{j=1}^{2J} \frac{qz - z_j}{1 + zz_j} - \frac{iz}{q} \prod_{j=1}^{2J} \frac{q^{-1}z - z_j}{1 + zz_j} \quad (36)$$

and taking the limit  $z \rightarrow 0$  we find

$$\lambda = \left\{ 1 - z \left[ \sum_{j=1}^{2J} \left( \frac{1}{z_j} + z_j \right) - iq - \frac{1}{iq} \right] \right\} \prod_{j=1}^{2J} z_j + \mathcal{O}(z^2), \quad (37)$$

where the right hand side must be  $z$ -independent. Then

$$\lambda = \prod_{j=1}^{2J} z_j \quad (38)$$

and

$$\sum_{j=1}^{2J} \left( \frac{1}{z_j} + z_j \right) = iq + \frac{1}{iq}. \quad (39)$$

Taking now the limit  $z \rightarrow \infty$  in (36) we find

$$\lambda^2 = 1 + i(q - q^{-1}) \sum_{j=1}^{2J} z_j + \mathcal{O}\left(\frac{1}{z}\right), \quad (40)$$

where again the right hand side is  $z$ -independent yielding

$$\lambda^2 = 1 + i(q - q^{-1}) \sum_{j=1}^{2J} z_j. \quad (41)$$

Using (39) we can rewrite (41) in the alternative

$$\lambda^2 = 3 - q^2 - q^{-2} - i(q - q^{-1}) \sum_{j=1}^{2J} \frac{1}{z_j}. \quad (42)$$

We have thus derived the relation among an eigenvalue and the roots of the corresponding polynomial. The roots are determined by (33). Once the roots of a polynomial are known, the corresponding eigenvalue can be calculated using any of (38), (41), (42).

**4.1. Comparison to Square Lattice.** Studying the case of square lattice the authors of [8] have arrived to the equation  $(X^+ + X^-)f = Ef$  which in the polynomial representation takes the form

$$i\left(\frac{1}{z} + qz\right)f(qz) - i\left(\frac{1}{z} + q^{-1}z\right)f(q^{-1}z) = Ef(z). \quad (43)$$

Substituting

$$f(z) = \prod_{j=1}^{2J} (z - z_j) \quad (44)$$

into (43) and setting  $z = z_n$  one obtains the Bethe ansatz equation

$$\frac{1 + qz_n^2}{1 + q^{-1}z_n^2} = \prod_{j=1}^{2J} \frac{q^{-1}z_n - z_j}{qz_n - z_j}. \quad (45)$$

Taking the limits  $z \rightarrow 0$  and  $z \rightarrow \infty$  one finds

$$E = i(q - q^{-1}) \sum_{j=1}^{2J} z_j. \quad (46)$$

There is another relation following from (43) which is not presented in [8]. Considering the limits  $z \rightarrow 0$  and  $z \rightarrow \infty$  in (43) and comparing the next-to-leading order terms we find

$$\sum_{j=1}^{2J} \left( z_j + \frac{1}{z_j} \right) = 0 \quad (47)$$

which is the analog of (39).

## 5. NUMERIC ANALYSIS

Let us discuss the results of numeric analysis of how the roots are distributed over the complex plane.

We first present the case of  $\frac{\Phi}{\Phi_0} = \frac{2}{89}$  where we have 89 eigenvalues and the corresponding 89 polynomials determined by (31). Each polynomial is of order of  $N - 1 = 88$ , *i.e.* for every eigenvalue we have 88 roots. For demonstrative purposes we present the root distributions for some characteristic cases, describing how the locations of roots depend on eigenvalues (Figure 2). For the eigenvalues of maximal magnitude the roots are depicted in the left panel, while the subsequent panels depict the roots corresponding to the eigenvalues of smaller magnitude. The right panel corresponds to the eigenvalue of minimal magnitude.

For the maximal value of  $\lambda^2$  the roots are arranged in two spirals related via the complex conjugation. Decreasing  $\lambda^2$  we observe the appearance of the new branch which is a circle to high accuracy. Further decrease of  $\lambda^2$  causes the conversion of spirals into another circle, and for the minimal value of  $\lambda^2$  the two circles become transformed into what is shown in the right panel.

We next present the case of  $\frac{\Phi}{\Phi_0} = \frac{30}{89} \approx \frac{1}{3}$  in Figure 3. For the maximal  $\lambda^2$  the roots are arranged into two groups: straight lines with equiangular separation of  $\pi/3$  and the six points indicated in blue. Few couples of points are somewhat deviated from the straight lines. This can be explained by relatively small value of  $N$ . Increasing  $N$  the deviation will presumably disappear. For the eigenvalues of less magnitude we observe that roots regroup from the straight lines into a hexagon and eventually, for the eigenvalue with

minimal magnitude we observe the almost-perfect hexagon. The points left beyond the hexagon might be treated as relic of the straight lines shown on left panel.

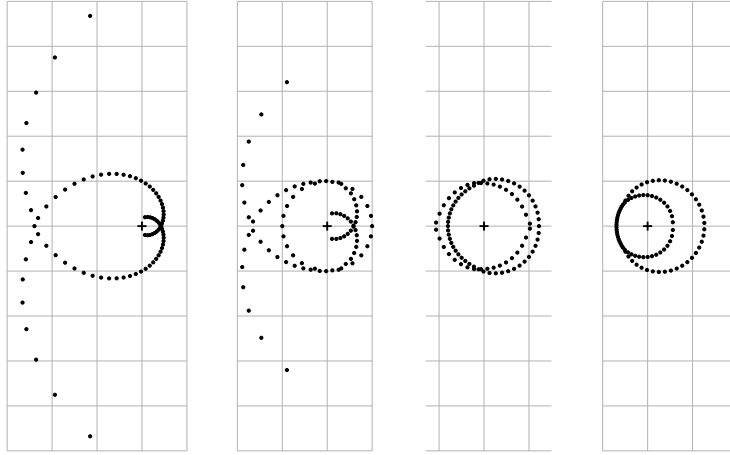


FIGURE 2. Root distributions on a complex plane for  $\frac{\Phi}{\Phi_0} = \frac{2}{89}$ .

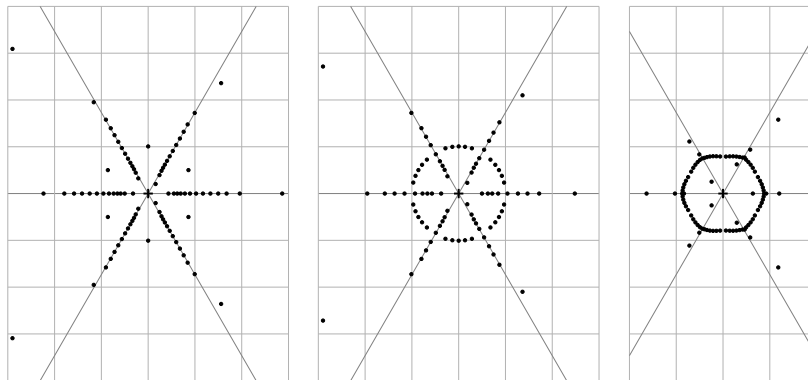


FIGURE 3. Root distributions on a complex plane for  $\frac{\Phi}{\Phi_0} = \frac{30}{89} \approx \frac{1}{3}$ .

We finally present the case of  $\frac{\Phi}{\Phi_0} = \frac{22}{89} \approx \frac{1}{4}$  in Figure 4. Interplay among the two groups of roots is again the case. One group consists of 8 straight lines with equiangular separation of  $\pi/4$ , and the other one resembling certain closed contour. Changing  $\lambda^2$  we observe that roots rearrange from

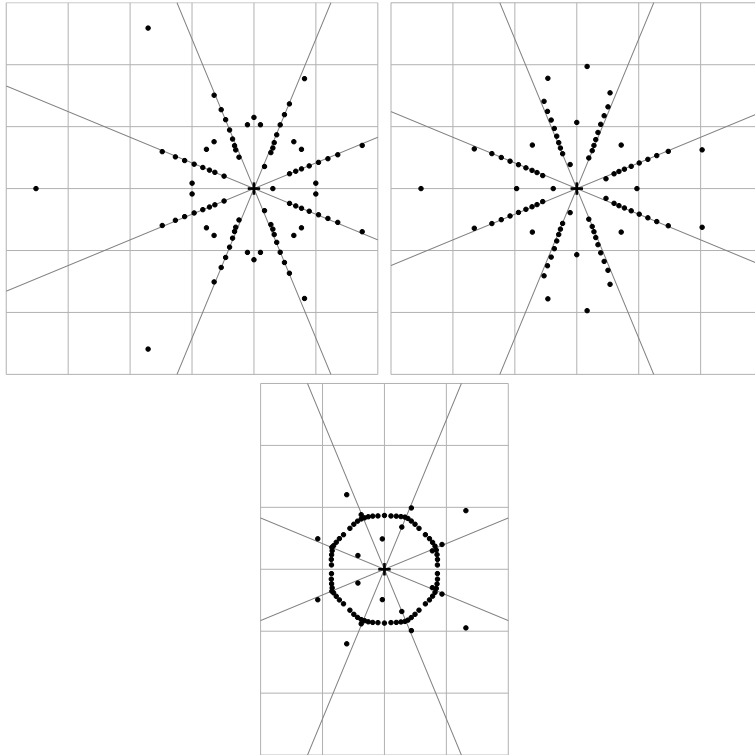


FIGURE 4. Root distributions on a complex plane for  $\frac{\Phi}{\Phi_0} = \frac{22}{89} \approx \frac{1}{4}$ .

one group into another and *vice versa*. For the lowest  $\lambda^2$  the roots are located basically on the aforementioned closed contour which appears to be an octagon as shown in the right panel.

## 6. CONCLUSIONS

We have considered the tight-binding model of spinless particles on a honeycomb lattice in magnetic field. The corresponding one-particle Hamiltonian turns out to be expressible in terms of the generators of the quantum group  $U_q(sl_2)$ . We have shown that varying the momentum  $\mathbf{k}$  the cyclic representation of  $U_q(sl_2)$  can be continuously deformed into the highest weight one. Involving the functional representation of  $U_q(sl_2)$  the Harper equation is reformulated as a system of functional equations which is subsequently reduced to a single equation (31) admitting solutions in the space of polynomials. Bethe-like equations determining the values of the roots

of polynomials is obtained and the locations of roots on the complex plane is investigated numerically. Using graphical plots we have shown that the roots distributions are highly organized and arranged in a regular geometric figures. Such observations make it clear that the analytic study of the equation (31), and of its symmetries in particular, would be of certain interest. This however, lays beyond the scope of a given account and is the matter of separate consideration.

#### APPENDIX A

The first Brillouin zone participating in (4) is usually drawn as a hexagon depicted in the left panel of Figure 5. For our purposes we rearrange it into the one shown in the right panel. The advantage of the rectangular one is that the limits of  $k_x$ -integration are independent of the value of  $k_y$  and *vice versa*.

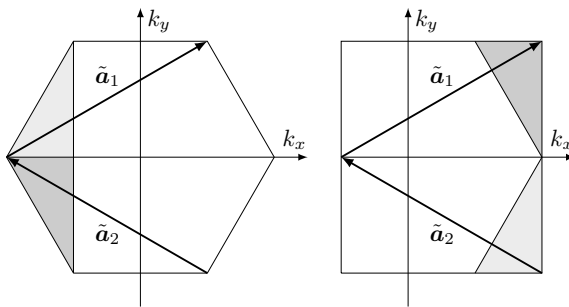


FIGURE 5. Left panel represents the first Brillouin zone. Using the vectors of equivalence  $\tilde{\mathbf{a}}_{1,2} = (\pm 1, \frac{1}{\sqrt{3}}) \frac{2\pi}{a}$  we rearrange the Brillouin zone into what is shown in the right panel.

Consider first the case of  $\nu = \text{even}$ . We then have

$$|\mathbf{k}_0| = \frac{\frac{1}{2}\nu}{N} \frac{4\pi}{\sqrt{3}a}, \quad (48)$$

where  $\frac{1}{2}\nu$  is integer, *i.e.*  $|\mathbf{k}_0|$  is the multiple of the  $N$ 'th part of the Brillouin zone. We then split the integration area in (4) into  $N$  horizontal strips of the height  $\frac{1}{N} \frac{4\pi}{\sqrt{3}a}$ . Introducing  $N$ -component vectors ( $\mu = A, B$ )

$$\Psi_\mu(\mathbf{k}) = \{c_\mu(\mathbf{k}), c_\mu(\mathbf{k} - \mathbf{k}_0), \dots, c_\mu(\mathbf{k} - N\mathbf{k}_0 + \mathbf{k}_0)\} \quad (49)$$

and combining  $\Psi_A$  and  $\Psi_B$  into  $\Psi = \{\Psi_A, \Psi_B\}$  we eventually come to (7).

In the case of  $\nu = \text{odd}$  we have to write (A1) as

$$|\mathbf{k}_0| = \frac{\nu}{2N} \frac{4\pi}{\sqrt{3}a} \quad (50)$$

i.e.  $|\mathbf{k}_0|$  is now the multiple of the  $(2N)$ 'th part of the Brillouin zone.

Performing the same steps as in the case of  $\nu = \text{even}$ , the magnetic Brillouin zone seems to be the  $\frac{1}{2N}$ 'th part of the original one. However this is not so and below we comment on the corresponding details.

We first split the integration area of (4) into  $(2N)$  equal horizontal strips and rewrite (4) as

$$H = \int_{\text{FBZ}/(2N)} \left\{ \mathbb{H}^\dagger(\mathbf{k}) + \mathbb{H}(\mathbf{k}) \right\} d\mathbf{k}, \quad (51)$$

where  $\text{FBZ}/(2N)$  denotes any separate strip and

$$\begin{aligned} \mathbb{H} = & \sum_{n=1}^{2N} c_A^\dagger(\mathbf{k} - n\mathbf{k}_0 + \mathbf{k}_0) c_B(\mathbf{k} - n\mathbf{k}_0 + \mathbf{k}_0) + \\ & + \sum_{n=1}^{2N} \xi_n(\mathbf{k}) c_A^\dagger(\mathbf{k} - n\mathbf{k}_0 + \mathbf{k}_0) c_B(\mathbf{k} - n\mathbf{k}_0) + \\ & + \sum_{n=1}^{2N} \zeta_n(\mathbf{k}) c_A^\dagger(\mathbf{k} - n\mathbf{k}_0) c_B(\mathbf{k} - n\mathbf{k}_0 + \mathbf{k}_0) \end{aligned} \quad (52)$$

with  $\xi_n(\mathbf{k}) = q^{-n} e^{i\mathbf{k}\mathbf{a}_1}$  and  $\zeta_n(\mathbf{k}) = q^{-n} e^{i\mathbf{k}\mathbf{a}_2}$ .

We then decouple the summations into  $1 \leq n \leq N$  and  $N+1 \leq n \leq 2N$  and introduce ( $\mu = A, B$ )

$$\begin{aligned} \chi_{\mu n}(\mathbf{k}) = & \frac{1}{\sqrt{2}} c_\mu(\mathbf{k} - n\mathbf{k}_0 + \mathbf{k}_0) + \\ & + \frac{(-1)^n i^N}{\sqrt{2}} c_\mu(\mathbf{k} - N\mathbf{k}_0 - n\mathbf{k}_0 + \mathbf{k}_0). \end{aligned} \quad (53)$$

We then construct

$$\Psi_\mu(\mathbf{k}) = \{ \chi_{\mu 1}(\mathbf{k}), \chi_{\mu 2}(\mathbf{k}), \dots, \chi_{\mu N}(\mathbf{k}) \} \quad (54)$$

and further  $\Psi = \{ \Psi_A, \Psi_B \}$  which leads to the same (7). In other words, the  $(2N)$  amount of modes involved in (A5) appear via the  $N$ -independent combinations (A6).

#### ACKNOWLEDGMENTS

We wish to thank A. Elashvili and M. Jibladze for helpful discussions. One of the authors (M.E.) is grateful to P. Sorba for illuminating communications. Research was supported in part by the Georgian NSF through the Grants No. ST09/09-280 (G.I.J) and ST08/4-405 (M.E., G.Ts.).

## REFERENCES

1. M. Ya. Azbel, Energy spectrum of a conduction electron in a magnetic field. (Russian) *Zh. Eks. Teor. Fiz.* **46** (1964), 929; English transl.: *Sov. Phys. JETP* **19**, (1964), 634.
2. D. R. Hofstadter, Energy levels and wave functions of Bloch electrons in rational and irrational magnetic fields, *Phys. Rev. B* **14** (1976), 2239.
3. F. Claro and G. H. Wannier, Magnetic subband structure of electrons in hexagonal lattices, *Phys. Rev. B* **19** (1979), 6068.
4. F. Claro, Spectrum of tight binding electrons in a square lattice with magnetic field, *Phys. Status Solidi (b)*, **104** K31 (1981).
5. Y. Hasegawa, P. Lederer, T. M. Rice and P. B. Wiegmann, Theory of electronic diamagnetism in two-dimensional lattices, *Phys. Rev. Lett.* **63** (1989), 907.
6. G. Semenoff, Condensed-Matter simulation of a three-dimensional anomaly, *Phys. Rev. Lett.* **53** (1984), 2449.
7. R. Rammal, Landau level spectrum of Bloch electrons in a honeycomb lattice, *J. Physique* **46** (1985), 1345.
8. P. B. Wiegmann and A. V. Zabrodin, Bethe-Ansatz for the Bloch electron in magnetic field, *Phys. Rev. Lett.* **72** (1994), 1980.
9. L. D. Faddeev and R. M. Kashaev, Generalized bethe ansatz equations for Hofstadter problem, *Commun. Math. Phys.* **169** (1995), 181.
10. Y. Hatsugai, M. Kohmoto and Y-Sh.Wu, Quantum group, Bethe ansatz equations, and Bloch wave functions in magnetic fields, *Phys. Rev. B* **53** (1996), 9697.
11. M. Kohmoto and A. Sedrakyan, Hofstadter problem on the honeycomb and triangular lattices: Bethe ansatz solution, *Phys. Rev. B* **73** (2006), 235118.
12. A. K. Geim and K. S. Novoselov, The rise of graphene, *Nature Materials* **6** (2007), 183.
13. C. Kassel, Quantum groups, *Graduate Texts in Mathematics*, vol. 155 Springer-Verlag, New York-Heidelberg-Berlin, 1995.
14. P. Roche and D. Arnaudon, Irreducible representations of the Quantum analogue of  $SU(2)^n$ , *Lett. Math. Phys.* **17** (1989), 295.

(Received 23.02.2012)

Authors' addresses:

M. Eliashvili

Iv. Javakhishvili Tbilisi State University  
 A. Razmadze Mathematical Institute  
 2, University str., Tbilisi 0186, Georgia  
 Department of Physics, Tbilisi State University  
 Chavchavadze Ave. 3, Tbilisi 0128, Georgia

G. Tsitsishvili

Department of Physics, Tbilisi State University  
 Chavchavadze Ave. 3, Tbilisi 0128, Georgia

G. Japaridze

Ilia State University, Cholokashvili Ave. 3–5, Tbilisi 0162, Georgia